Upsala Journal of Medical Sciences. 2015; 120: 144–156

informa
healthcare

ORIGINAL ARTICLE

Targeted deletion of *Vglut2* expression in the embryonal telencephalon promotes an anxiolytic phenotype of the adult mouse

KARIN NORDENANKAR, ASSAR BERGFORS & ÅSA WALLÉN-MACKENZIE

Department of Neuroscience, Unit of Functional Neurobiology and Unit of Developmental Genetics, Uppsala University, Box 593, S-75214 Uppsala, Sweden

Abstract

Background. Anxiety is a natural emotion experienced by all individuals. However, when anxiety becomes excessive, it contributes to the substantial group of anxiety disorders that affect one in three people and thus are among the most common psychiatric disorders. Anxiolysis, the reduction of anxiety, is mediated via several large groups of therapeutical compounds, but the relief is often only temporary, and increased knowledge of the neurobiology underlying anxiety is needed in order to improve future therapies.

Aim. We previously demonstrated that mice lacking forebrain expression of the *Vesicular glutamate transporter 2* (*Vglut2*) from adolescence showed a strong anxiolytic behaviour as adults. In the current study, we wished to analyse if removal of *Vglut2* expression already from mid-gestation of the mouse embryo would give rise to similar anxiolysis in the adult mouse.

Methods. We produced transgenic mice lacking *Vglut2* from mid-gestation and analysed their affective behaviour, including anxiety, when they had reached adulthood.

Results. The transgenic mice lacking *Vglut2* expression from mid-gestation showed certain signs of anxiolytic behaviour, but this phenotype was not as prominent as when *Vglut2* was removed during adolescence.

Conclusion. Our results suggest that both embryonal and adolescent forebrain expression of *Vglut2* normally contributes to balancing the level of anxiety. As the neurobiological basis for anxiety is similar across species, our results in mice may help improve the current understanding of the neurocircuitry of anxiety, and hence anxiolysis, also in humans.

Key words: *Affective, anxiolysis, behaviour, development, psychostimulant*

Introduction

Glutamate is the main excitatory neurotransmitter in the mammalian brain, and glutamatergic transmission is solidly regulated both pre-and post-synaptically during healthy conditions. Dysregulated glutamatergic transmission is implicated in several neuropsychiatric disorders, including schizophrenia, addiction and anxiety disorders (for examples of recent reviews see (1-4)). Better understanding of the neurobiology and neurocircuitry of glutamatergic neurons is therefore needed to identify future potential therapeutic targets.

The presence of vesicular glutamate transporters (VGLUTs) 1 and/or 2 (encoded by the *Vglut1* and *Vglut2* genes, aka *Slc17A7* and *Slc17A6*, respectively) defines the presynaptic glutamate site (5-10). Expression analyses of the adult telencephalic area in the mouse and rat have shown a strong predominance for *Vglut1* mRNA across the cerebral cortex and hippocampus, areas in which *Vglut2* is only found regionally distributed. More specifically, *Vglut2* mRNA is

Correspondence: Åsa Wallén-Mackenzie, Department of Neuroscience, Unit of Functional Neurobiology and Unit of Developmental Genetics, Uppsala University, Box 593, 751 24 Uppsala, Sweden. Fax: +46 18 511 540. E-mail: asa.mackenzie@neuro.uu.se

(Received 15 January 2015; accepted 13 March 2015)

ISSN 0300-9734 print/ISSN 2000-1967 online © 2015 Informa Healthcare
DOI: 10.3109/03009734.2015.1032454

localized to the retrosplenial group (RSG), layers III and V/VI of the neocortex, and to the endo-piriform cortex. Within the hippocampal formation, the expression is confined to the subiculum (7,9,11-13). Both *Vglut1* and *Vglut2* mRNAs are found in the olfactory bulb (14), and both are localized to the amygdaloid complex, albeit to different subpopulations. *Vglut2* mRNA is detected only in the medial (Me), anterior cortical (ACo), and anterior basomedial (BM) nuclei, while *Vglut1* mRNA is found in all other amygdaloid populations (13,15). *Vglut2*, the predominant *Vglut* in deep structures of the adult brain, is broadly distributed already at mid-gestation of the developing mouse embryo (16,17). This expression is subsequently down-regulated in most areas postnatally populated by *Vglut1* mRNA (7-9,18-20).

Behavioural phenotyping of mice gene-targeted for either *Vglut1* or *Vglut2* has implied a role for the presynaptic glutamate site in behaviour of relevance for psychiatric conditions. Mice heterozygous for *Vglut1*, the predominant *Vglut* in the telencephalon, showed an anxiogenic phenotype as well as depression- and schizophrenia-related behaviours (21,22). Demonstrating the importance of *Vglut2* in the brainstem, a full knock-out of *Vglut2* led to immediate neonatal lethality due to respiratory failure (23,24). By using the Cre/LoxP conditional gene targeting system (reviewed in (25)), the functional role of VGLUT2 in neuropsychiatric-like conditions has been further addressed. For example, several studies of mice gene-targeted specifically for *Vglut2* within dopamine neurons (26) have demonstrated alterations in the response to psychostimulants, leading to a proposed role of VGLUT2 in mechanisms of importance for addiction (16,17,27-29). The regional distribution of *Vglut2* in the forebrain was previously targeted in our laboratory at the adolescent stage by use of the CamKIIα-Cre transgenic mouse line, which can be detected from postnatal week 3 (30). By behavioural and biochemical analysis of adult $Vglut2^{f/f;CaMKII\text{-}Cre}$ conditional knock-out (cKO), we identified an anxiolytic phenotype alongside several behaviours relevant for animal models of schizophrenia (13). In the current study, we aimed to approach whether *Vglut2* gene expression during embryo development is of any relevance for affective behaviour at adulthood. To analyse this issue, we used the previously described $Emx1^{IRES\text{-}Cre}$ knock-in mice (31) to drive dorsal telencephalic deletion of *Vglut2* expression from mid-gestation onwards. We analysed adult $Vglut2^{f/f;Emx1\text{-}Cre}$ cKO and control mice for functions of relevance to psychiatric conditions, including measures of psychostimulant-induced behavioural activation, sociability, and various aspects of anxiety.

Material and methods

Animals

All mice used in the study were housed in the animal facility at the BMC, Uppsala University, in accordance with the Swedish regulation guidelines (Animal Welfare Act SFS 1998:56) and European Union legislation (Convention ETS123 and Directive 2010/63/EU). Ethical approval was obtained from the Uppsala Animal Ethical Committee. Mice were housed at constant temperature (21 ± 1°C) and humidity (50%–60%) with 2–8 mice per cage unless otherwise stated. All behavioural experiments took place during the light phase, between 06.00 and 18.00. Food (R3, Lactamin/Lantmännen, Sweden) and water were provided *ad libitum* unless otherwise stated. All behaviour tests were performed on adult (>10 weeks) mice.

Generation of $Vglut2^{f/f;Emx1\text{-}Cre}$ mice

The $Vglut2^{f/f;Emx1\text{-}Cre}$ mouse line was produced by using the breeding procedure established for conditional knock-out mice to ensure identical genetic background (32). By crossing mice homozygous for the floxed allele of *Vglut2* ($Vglut2^{f/f}$) (24) with $Emx1^{IRES\text{-}Cre}$ knock-in mice (31), hereafter referred to as Emx1-Cre mice, both $Vglut2^{f/f;Emx1\text{-}Cre(tg/wt)}$ conditional knock-out mice (cKO) and $Vglut2^{f/f;Emx1\text{-}Cre(wt/wt)}$ control mice (which do not express the *Emx1-Cre* transgene and therefore have normal *Vglut2* expression) were produced as littermates which allows for behavioural phenotyping and comparison between genotype groups (33). The $Vglut2^{f/f;Emx1\text{-}Cre}$ cKO and ctrl mice were thus of the same genetic background, a mixture of C57/BL6 and Sv129. Genotyping was performed as previously described (24).

Tissue sectioning and RNA probes

Mice were intraepidermally injected with a 1:1 mixture of Dormitor (medetomidine hydrochloride, 70 μg/g body weight; Orion Pharma, Espoo, Finland) and Ketalar (ketamine hydrochloride, 7 μg/g body weight, Pfizer, Groton, CT, USA). Transcardial perfusion was performed with phosphate-buffered saline (PBS) followed by 4% formaldehyde (HistoLab, Västra Frölunda, Sweden). The brain was excised and stored in 4% formaldehyde overnight, after which it was washed in PBS and embedded in 4% agarose and sectioned (70 μm) on a Leica VT1000S Vibratome (Leica Biosystems, Nussloch, Germany). Sections were dehydrated through a series of methanol washes (25%, 50%, and 75% methanol) and

lastly stored in 100% methanol at –20°C until further processing.

Templates for *in situ* probes were derived from commercial cDNA clones by using gene-specific promotors (as described at www.genepaint.org). The *Vglut2* probe covers nucleotides (nts) 1616-2203 (NM_080853.2), the *Vglut1* probe nts 462-1067 (NM_182993), and the vesicular inhibitory amino acid transporter (*Viaat*) probe nts 1578-1889 (NM_009508.1). The probes were synthesized by using T7, T3, or Sp6 RNA polymerase in the presence of digoxigenin-11-UTP (Roche Diagnostics Scandinavia, Stockholm, Sweden). Probes were controlled and quantified by using the NanoDrop ND-1000 Spectrophotometer (NanoDrop Technologies, Wilmington, DE, USA).

In situ hybridization on free-floating sections

Mouse brain sections were step-wise rehydrated from 100% methanol to PBT (PBS with 0.1% Tween-20 (Sigma-Aldrich Sweden AB, Stockholm, Sweden)) and bleached in 6% hydrogen peroxidase in PBT. Thereafter, the sections were permeabilized with 0.5% TritonX-100 (Sigma-Aldrich Sweden AB, Stockholm, Sweden), digested with 20 µg/mL proteinase K (Invitrogen, Nordic Biolabs, Täby, Sweden) and post-fixed in 4% formaldehyde (Histo-Lab) with PBT washes between all steps. Sections were then pre-hybridized at 55°C in hybridization buffer (50% formamide, 5 × SSC, pH 4.5, 1% SDS, 50 µg/mL of tRNA (Sigma), 50 µg/mL of heparin (Sigma), and PBT). The digoxigenin-labelled probe (1 µg/mL) diluted in hybridization buffer was heat-denatured at 80°C, cooled on ice, and added to the sections for hybridization overnight at 55°C (14–16 h). Unbound probe was removed by sequential washes of buffer 1 (50% formamide, 5 × SSC, pH 4.5, and 1% SDS in PBT) followed by buffer 2 (50% formamide, 2 × SSC, pH 4.5, and 0.1% Tween-20 in PBT) at 55°C. The sections were further washed in 0.1% Tween-20 Tris-buffered saline (TBST) before incubation in blocking solution (1% blocking reagent (Roche Diagnostics Scandinavia, Stockholm, Sweden)) together with 1:5,000 diluted anti-digoxigenin alkaline phosphates conjugated antibody (Roche Diagnostics Scandinavia) overnight at 4°C. Unbound antibody was removed by sequential washes with 2 mM levamisole (GTF Fisher, Stockholm, Sweden) in TBST followed by washes with 2 mM levamisole in NTMT (100 mM NaCl, 10 mM Tris-HCl, pH 9.5, 50 mg $MgCl_2$, and 0.1% Tween-20). Sections were developed in BM purple AP substrate (Roche Diagnostics Scandinavia) at 37°C. After mounting in glycerol, the sections were photographed in a Leica MZ16F dissection microscope using a DFC300FX camera and FireCam software (Leica Microsystem). Images were adjusted in Adobe Photoshop CS3 (San Jose, CA, USA) by adjusting the levels and brightness/contrast. Figures were assembled in Adobe Illustrator CS3.

Ethical considerations

The number of mice used in the study was reduced by allowing one batch of mice ($n = 17$ Ctrl; $n = 12$ cKO) for analysis in the elevated plus maze (EPM), the multivariate concentric square field™ (MCSF), the social interaction, and the dominance tube test in this order, before being processed for dissection and monoamine analysis by high-pressure liquid chromatography (HPLC). Two separate batches of mice were analysed in the Porsolt forced swim test ($n = 19$ Ctrl; $n = 13$ cKO) and in an amphetamine provocation set-up ($n = 9$ Ctrl; $n = 9$ cKO), respectively.

Amphetamine challenge

Amphetamine-induced activity was analysed in automated activity boxes, so-called locoboxes (Locobox, Kungsbacka Reglerteknik AB, Kungsbacka, Sweden) that each consists of a plastic cage (55 × 55 × 22 cm) placed inside a ventilated and illuminated (10 lux) cabinet. Inside the locobox, a grid of photo beams (beams spaced by 5 cm) records the movement of the mouse. On the first experimental day, each mouse was allowed to explore the cage for 30 min in order to measure baseline activity, and was thereafter injected with 10 mL/kg saline (i.p.) and allowed back to the locobox for an additional 90 min of monitoring. Twenty-four hours later, the same protocol was used, but instead of saline the mice were injected i.p. with 1.5 mg/kg of amphetamine. The locobox-parameters scored were locomotion, peripheral activity, and corner activity as previously described (16). Locomotion is defined by two beam breaks anywhere in the box; peripheral activity is defined by two beam breaks in the periphery of the box; corner activity is defined by two beam breaks in any of the four corners of the box. Data were analysed by two-way ANOVA by Prism software (GraphPad) (variables: genotype, cKO versus ctrl; time, 30 min for pre-injection and 90 min for post-injection).

EPM, MCSF, and social interaction analyses followed by monoamine analysis

The behavioural set-ups for the EPM, MCSF, social interaction, and social dominance tests, performed in this order, have been described previously (13). After cervical dislocation, brains were rapidly dissected and mounted into a coronal mouse brain matrix (Ted Pella,

Inc., Redding, CA, USA) kept on ice from which 1-mm slices were prepared. The nucleus accumbens, dorsal striatum, hippocampus, and prefrontal cortex (PFC) from cKO mice and littermate controls were microdissected from these slices. Samples were instantly frozen on dry ice and kept frozen at −80°C until analysis. After ultrasound homogenization (Sonifier Cell Disruptor B30, Branson Ultrasonics, Danbury, CT, USA) in 0.1 M perchloric acid containing 2.5 mM of Na_2EDTA and subsequent centrifugation (10,000 rpm, 10 min), the supernatant was collected for analysis. The supernatant was removed, and the pellet washed with double-distilled water three times. A mixture of 0.2 M acetic acid and 0.2 M phosphoric acid (8:2, vol/vol) was added, and samples were shaken again for 15 minutes. The eluate was analysed for dopamine (DA), 3,4-dihydroxyphenylacetic (DOPAC) and noradrenaline (NA), 3-methoxytyramine (3-MT) and serotonin (5-HT) using HPLC with electrochemical detection as previously described (13,34,35).

The Porsolt forced swim test

The Porsolt swim test represents a model for interpretation of animal depression-like behaviour (36,37). Each mouse was placed in a plexiglas cylinder (Ø20 cm) filled with 25 ± 2°C water. The mice were videotaped during two consecutive 12-minute trials with 24 hours in between and scored (Ani-Tracker Software) for total time spent swimming (defined as at least three paws paddling).

Statistical analysis

A non-parametric Mann–Whitney *U* test was used for statistical analyses of differences between genotype groups (behaviour and monoamine content) except in the case of behaviour analyses over time when two-way ANOVA or repeated measures two-way ANOVA were implemented. Multiple testing included Bonferroni's *post-hoc* comparisons unless otherwise stated. The chi-square test was used for statistical comparison in the elevated plus maze to evaluate the difference in the number of mice entering and not entering the outer open arm. Values in graphs are expressed as mean ± SEM.

Results

Conditional deletion of Vglut2 expression in the olfactory bulb, cortex, hippocampus, and part of the amygdala complex

The Emx1-driven Cre activity in the $Emx1^{IRES\text{-}Cre}$ knock-in mouse line was investigated previously by reporter-gene analysis of the R26R strain and shown to be dorsally located in cortical subdivisions of the telencephalon from embryonic day (E) 10.5 and to stay regionally distributed also in the adult telencephalic area (31). Areas characterized by Emx1-driven Cre activity in the adult included the whole neocortex and the entire hippocampal formation as defined by the subiculum, hippocampus proper, and the dentate gyrus. The olfactory bulb and several, but not all, subpopulations of the amygdala were also characterized by Emx1-driven Cre activity. Cre-active areas included the lateral (L), centrolateral (CL), basolateral (BL), and basomedial (BM) amygdala, while leaving untouched the adjacently located medial (Me) and central (C) amygdaloid nuclei as well as the bed nucleus of stria terminalis (Bst) (the two last-mentioned a part of the so-called extended amygdala). Somewhat weaker activity was detected in the anterior cortical (ACo) amygdala (31). Guided by this previous report, brain sections from $Vglut2^{f/f;Emx1\text{-}Cre(tg/wt)}$ cKO mice and littermate $Vglut2^{f/f;Emx1\text{-}Cre(wt/wt)}$ control mice, produced as described in 'Materials and methods', were analysed by *in situ* hybridization (ISH) at the adult stage in order to ascertain the targeted deletion of *Vglut2*. As we previously reported, expression of *Vglut2* in the adult telencephalon was found in the retrosplenial group (RSG) and layers III and V/VI (Figure 1E, Q) (13). Expression was also found in the mitral and deep periglomerular cells of the olfactory bulb (Figure 1A, I), much resembling the expression previously reported in the rat olfactory system during embryonal development (14). In accordance with the reported Cre-activity of the $Emx1^{IRES\text{-}Cre}$ mouse line (31), *Vglut2* mRNA expression was found deleted in all of these telencephalic areas in the cKO brains (Figure 1R, E, B and J). Further, as described before, *Vglut2* expression in controls was evident in the subiculum, but not in the rest of the hippocampal formation (Figure 1Q), and in several subnuclei of the amygdala complex, including the ACo, the BM, and anterior and posteroventral Me nuclei (Figure 1M, O). In the cKO mice, the subicular and BM *Vglut2* expression was found absent, again in accordance with the reported Cre activity (Figure 1R, N) (31). However, *Vglut2* expression in the ACo appeared reduced only (Figure 1N), in line with the limited Cre activity described in this area (31), while the expression in the Me appeared normal, fitting the apparent lack of Cre activity in these areas (Figure 1N, P) (31). In addition, we addressed *Vglut2* expression in all of the remaining brain and found it normal compared to control mice (Figure 1G, H; Table I) (Supplementary Table S1, available online). Thus, in the adult $Vglut2^{f/f;Emx1\text{-}Cre(tg/wt)}$ cKO mice,

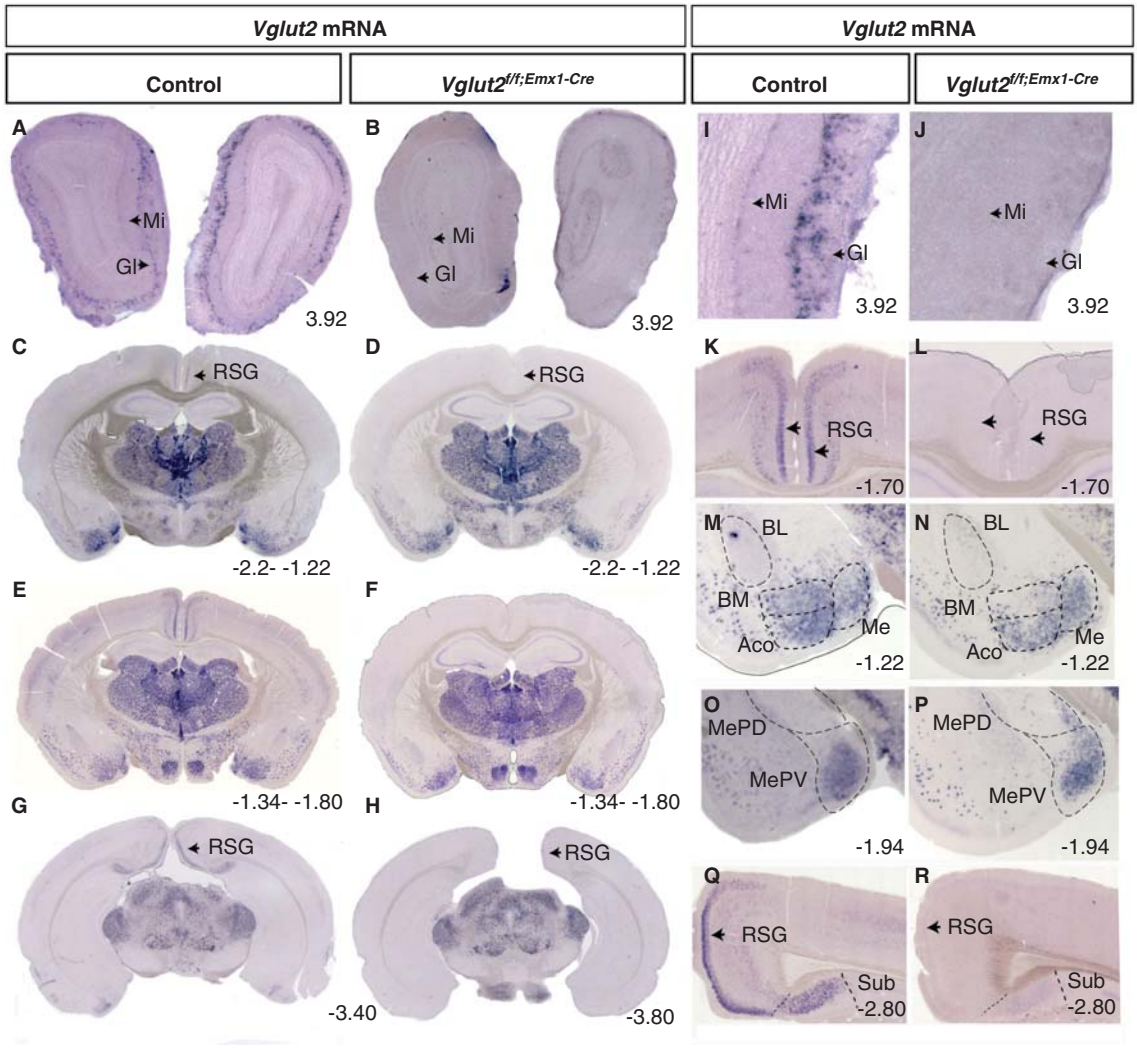

Figure 1. Specific deletion of *Vglut2* in selected forebrain target areas. Floating *in situ* hybridization on coronal brain (70 μm) sections from control mice and *Vglut2*$^{f/f;Emx1\text{-}Cre}$ cKO mice (A–H) using a DIG-labelled *Vglut2* probe. Close-ups as indicated in I–R, which demonstrate that cells expressing *Vglut2* mRNA was absent in the mitral cell (Mi) layer and GI layer in the olfactory bulb (I–J). *Vglut2* mRNA was also absent in the RSG of the medial cortex in the *Vglut2*$^{f/f;Emx1\text{-}Cre}$ mice (K, L). There is a loss of *Vglut2* mRNA in the BMA, in the ACo the mRNA is partially deleted, and the Me amygdala and MePV are unaltered in the *Vglut2*$^{f/f;Emx1\text{-}Cre}$ mice (M–P). *Vglut2* mRNA positive cells were present in the Sub in control mice but not in *Vglut2*$^{f/f;Emx1\text{-}Cre}$ cKO mice (Q, R). ACo = anterior cortical amygdaloid area; BL = basolateral amygdaloid nucleus; BM = basomedial amygdaloid nucleus anterior part; cKO = conditional knock-out; DIG = digoxigenin; GI = periglomerular layer; Me = medial amygdaloid nucleus; MePV = posteriorventral medial amygdaloid nucleus; Mi = mitral cell layer; RSG = retrosplenial group; Sub = subiculum; Bregma interval (dorsal, ventral) is shown in lower right corner.

the targeted deletion of *Vglut2* is specific to the olfactory bulb, cortical subregions, the subiculum, and the BM and ACo areas of the amygdala, regions that all express the *Emx1*$^{IRES\text{-}Cre}$ bicistronic construct.

Normal overall histology and distribution of cellular marker genes

To verify that the overall brain anatomy was normal in the *Vglut2*$^{f/f;Emx1\text{-}Cre(tg/wt)}$ cKO mice, ISH analysis of one additional glutamatergic marker, *Vglut1*, and of one marker for inhibitory neurons, the vesicular amino acid transporter (*Viaat*), was performed. In contrast to the restricted expression of *Vglut2* in the telencephalon, *Vglut1* is prominently expressed in this area (7,9,11-13,38). Strong *Vglut1* expression was found throughout the neocortex and hippocampal formation and also in several subnuclei of the amygdala complex (Figure 2A, C), which is in accordance with previous studies. *Vglut1* was most prominently expressed in the BL, BM, and Me nuclei of the amygdala. No altered distribution was seen in the cKO brains (Figure 2B, D; and data not shown). Further, expression of *Vglut1* in the mid-brain,

Table I. Summarized results from *in situ* hybridization evaluating the presence or not of *Vglut2* mRNA in brain structures from three adult *Vglut2*$^{f/f;Emx1\text{-}Cre}$ cKO mice and three control mice.

	Structure	Ctrl	cKO
Pallium	Neocortex	+	–
	RSG	+	–
	Subiculum	+	–
	Hippocampus CA1, CA3, DG	–	–
	Septohippocampus	–	–
	Ventral endopiriform nucleus	+	–*
	Piriform cortex	+	–*
	Claustrum	+	–*
Border regions	Lateral septum	–	–
	Medial septum	–	–
	Rostroventral septum	–	–
	Endopiriform nucleus	–	–
	Lateral amygdala	–	–
	BM	+	–*
	Me	+	+
	ACo	+	–*
Subpallium	Olfactory tuberculum	+	+
	Striatum	–	–
	Ventral pallidum	–	–
	Nucleus accumbens	ND	ND
	Bed nucleus stria terminalis	ND	ND
	Lateral olfactory tract	ND	ND
Olfactory bulb	Mitral cell layer	+	–
	External plexiform	–	–
	Internal plexiform	–	–
	Periglomerular layer	+	–*
	Granule cell	–	–
	Ependymal layer	–	–

The expression for the Emx1-Cre transgene was described previously (Gorski et al. 2002 (31)), and those structures in which Emx1-Cre was there shown to be expressed were analysed for *Vglut2* mRNA and listed here.
+ = expression of *Vglut2* mRNA Emx1-Cre transgene; – = no expression; –* = low amounts of expression; cKO = conditional knock-out; DG = dentate gyrus; ND = not determined.

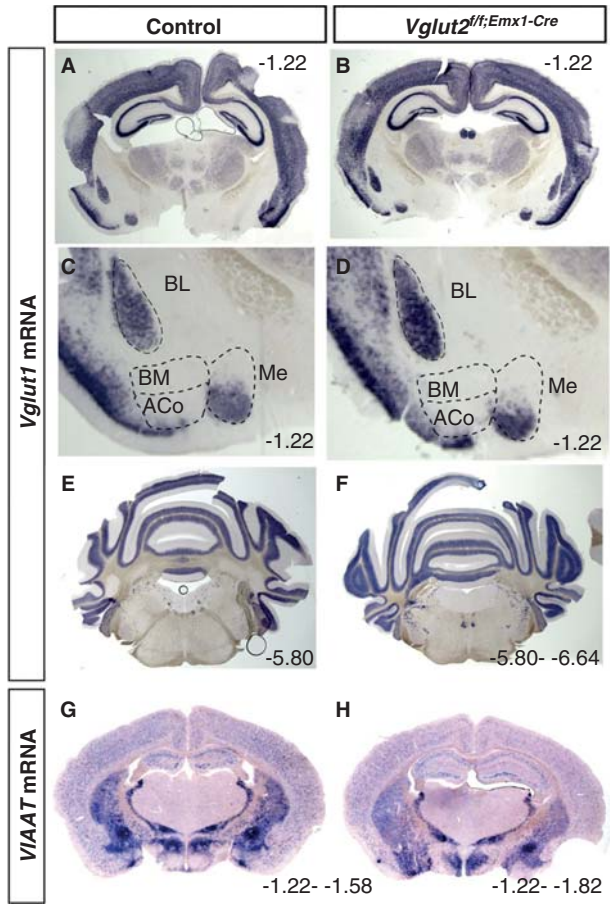

Figure 2. **Verification that the overall gross anatomy is normal in the *Vglut2*$^{f/f;Emx1\text{-}Cre}$ mice compared to control mice.** Floating *in situ* hybridization on coronal brain (70 μm) sections from control and *Vglut2*$^{f/f;Emx1\text{-}Cre}$ cKO mice using a DIG-labelled *Viaat* (A, B) or *Vglut1* (C–H) probe. Close-ups show that ACo and BM do not express *Vglut1* mRNA, while BL and part of Me express *Vglut1* mRNA. ACo = anterior cortical amygdaloid area; BL = basolateral amygdaloid nucleus; BM = basomedial amygdaloid nucleus anterior part; Me = medial amygdaloid nucleus. Bregma interval (dorsal, ventral) is shown in lower right corner.

cerebellum, and pons appeared normal in the cKO brains compared to controls (Figure 2E, F). *Viaat* expression was also detected, as expected, in inhibitory populations and appeared normal in the cKO brain compared to controls (Figure 2G, H). Together, these results showed normal cellular distribution of excitatory and inhibitory populations in the *Vglut2*$^{f/f;Emx1\text{-}Cre(tg/wt)}$ cKO mice, and although this was not quantitative, by ISH analysis, we did not detect differences in expression levels in these areas.

Normal basal and amphetamine-induced activity in agreement with unaltered DA levels

The behavioural analyses of the previously reported *Vglut2*$^{f/f;CaMKII\text{-}Cre}$ cKO mice revealed a spontaneous hyperactivity which was further accentuated above the levels of the controls when mice were challenged with an acute dose of amphetamine (13). This increased behavioural activation was correlated with increased basal levels of dopamine in the striatum, which we suggested as the underlying cause of the hyperactivity (13), in accordance with the role of dopamine in

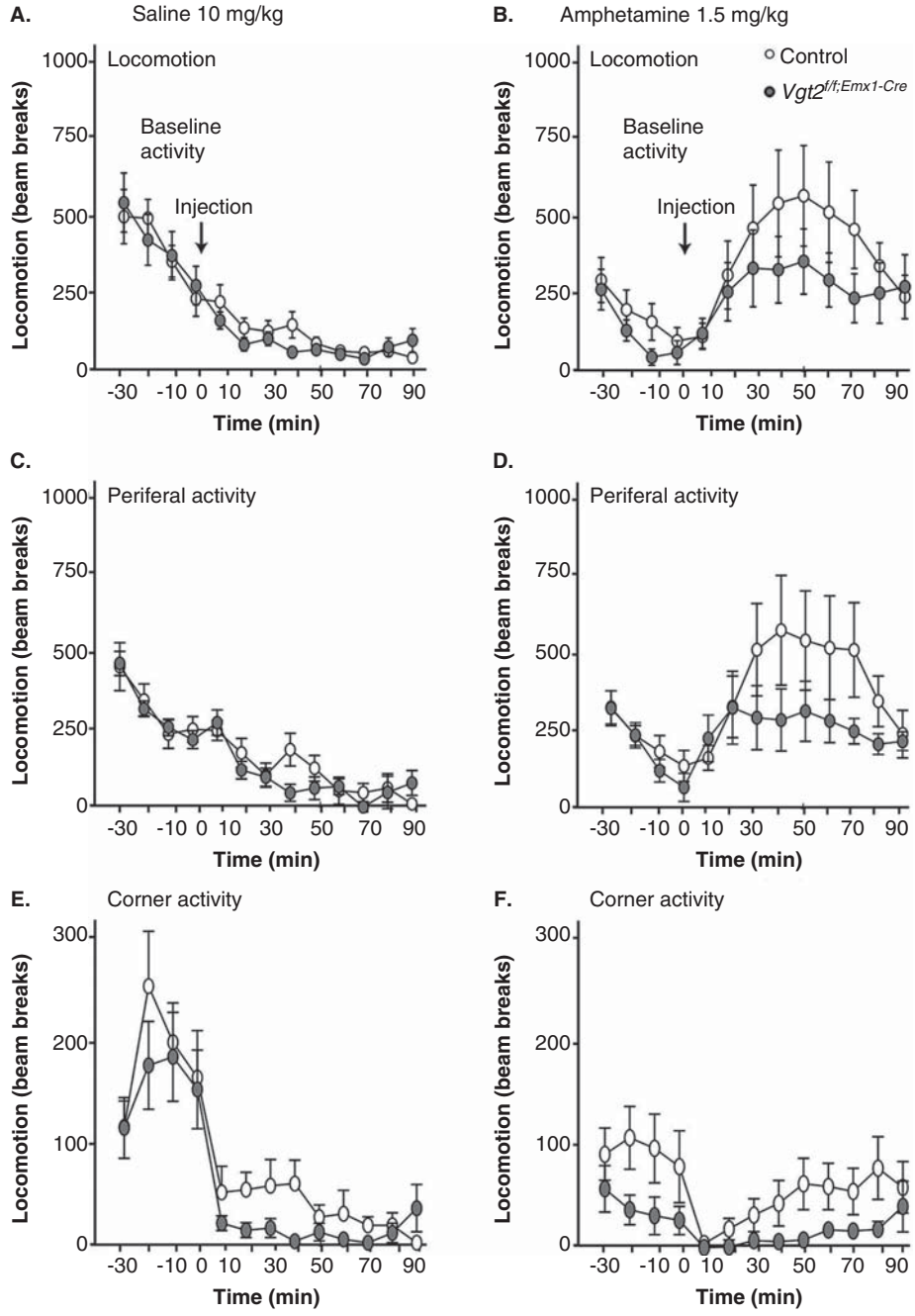

Figure 3. The *Vglut2*$^{f/f;Emx1\text{-}Cre}$ mice do not show any altered response to amphetamine. The initial response to novel environment (30 min) and overall response after i.p. injection of saline (90 min), 10 mg/kg, in locomotion, periferal activity, and corner activity are unaltered in the *Vglut2*$^{f/f;Emx1\text{-}Cre}$ cKO mice compared to control mice (B, D, F). On day 2, the mice were subjected to the activity boxes for 30 min and were thereafter administered 1.5 mg/kg amphetamine i.p. and were recorded for 90 min (A, C, E). The arrows in the graphs depict the time of saline and amphetamine injection. Data were analysed with two-way ANOVA and showed no significant interactions (effect of genotype). Data are represented as mean ± SEM. cKO = conditional knock-out.

general activational response (39). Caretaker handling of the *Vglut2*$^{f/f;Emx1\text{-}Cre(tg/wt)}$ cKO mice now revealed that these mice were calmer than the *Vglut2*$^{f/f;CaMKII\text{-}Cre}$ cKO mice, which we previously had experienced as difficult to handle due to the strong hyperactivity. This observation tentatively suggested that the telencephalic deletion of *Vglut2* from embryo development (*Vglut2*$^{f/f;Emx1\text{-}Cre}$ cKO) had a different effect on behaviour than had the postnatal deletion (*Vglut2*$^{f/f;CaMKII\text{-}Cre}$ cKO). By comparing spontaneous and amphetamine-induced activity between the *Vglut2*$^{f/f;Emx1\text{-}Cre}$ cKO mice and their

Table II. Levels of monoamines and dopamine metabolites (ng/g of wet tissue) of *Vglut2*$^{f/f;Emx1\text{-}Cre}$ cKO ($n = 12$) and control ($n = 18$) mice. The data show no statistically significant alterations between control and cKO mice. Data are presented as mean ± SEM.

Brain region	Metabolite	Ctrl	*Vg2*$^{f/f;Emx1\text{-}Cre}$	*P* value
Nucleus accumbens	Dopamine	0.0129 ± 9.1E-04	0.0122 ± 9.5E-04	0.21
	DOPAC	0.0053 ± 3.9E-04	0.0049 ± 5.7E-04	0.48
	DOPAC/DA	0.4784 ± 3.6E-02	0.4708 ± 4.6E-02	0.99
	NA	0.0015 ± 2.1E-04	0.0015 ± 3.1E-04	0.82
	3-MT	0.0032 ± 2.7E-04	0.0025 ± 2.9E-04	0.26
	5-HT	0.0040 ± 3.1E-04	0.0030 ± 3.8E-04	0.15
Caudatus putamen	Dopamine	0.0197 ± 1.4E-03	0.0200 ± 2.2E-03	0.08
	DOPAC	0.0059 ± 5.2E-04	0.0066 ± 7.0E-04	0.51
	DOPAC/DA	0.3386 ± 4.7E-02	0.2958 ± 2.1E-02	0.47
	NA	0.0004 ± 8.0E-05	0.0003 ± 4.7E-05	0.51
	3-MT	0.0038 ± 5.0E-04	0.0045 ± 4.8E-04	0.36
	5-HT	0.0012 ± 2.2E-04	0.0015 ± 2.1E-04	0.24

$P < 0.05$ (Mann–Whitney *U* test).
Nucleus accumbens corresponds to the ventral striatum; Caudatus putamen to the dorsal striatum.
3-MT = 3-methoxytyramine; 5-HT = 5-hydroxytryptamine; cKO, conditional knock-out; DOPAC = 3,4-dihydroxypheneylacetic acid; NA = noradrenalin.

littermate control mice, no statistically relevant difference in either locomotion, corner activity, or peripheral activity was detected between genotypes either pre- or post-injection by saline or amphetamine (Figure 3A–F) (all statistical data are shown in Supplementary Table S2, available online). Further, we did not find any weight differences between either male (ctrl $n = 11$, 30.4 ± 0.7 g; cKO $n = 6$, 28.7 ± 0.4 g, $P = 0.13$) or female mice ($n = 10$, 22.1 ± 0.8 g; cKO $n = 8$, 22.5 ± 0.9 g, $P = 0.75$) of the different genotype groups, indicating normal food intake and activational levels in the cKO mice. Biochemical detection of DA and its metabolite DOPAC as well as noradrenalin, 3-MT, and 5-HT in tissue dissected from the dorsal (caudate putamen) and ventral (nucleus accumbens) striatum did not reveal any differences between the *Vglut2*$^{f/f;Emx1\text{-}Cre(tg/wt)}$ cKO and control mice (Table II). Taken together, these results show that adult mice lacking *Vglut2* in selected telencephalic areas from early developmental stages show normal spontaneous and amphetamine-induced activity as well as normal levels of monoamines DA, NA, 5-HT, and their metabolites in the striatum.

Decreased avoidance of open areas and time spent in shelter suggest an anxiolytic phenotype

Altered social skills, as measured by the social interaction test and the dominance tube test, were part of the behavioural phenotypes described for the *Vglut2*$^{f/f;CaMKII\text{-}Cre}$ cKO (13). By using the same paradigms here, no differences between the *Vglut2*$^{f/f;Emx1\text{-}Cre(tg/wt)}$ cKO and control mice were detected either in the social interaction test ($P = 0.85$) or in the dominance tube test ($P = 0.58$) (Figure 4A, B). Also, no difference between genotype groups could be discerned in the Porsolt forced swim test, a model for despair-like behaviour (trial 1, $P = 0.86$; trial 2 $P = 0.54$) (Figure 4C), which previously revealed an altered response in the *Vglut2*$^{f/f;CaMKII\text{-}Cre}$ cKO mice (13). Behavioural analysis of relevance to anxiety in humans include an apparatus which takes into advantage the rodent's preference for familiar, dark, and/or enclosed areas (40). The EPM, which allows exploration of open versus enclosed areas is perhaps the most commonly used such method. The MCSF, which contains multiple challenges including both an open field and a dark, sheltered space, as well as challenges related to risk-assessment and risk-taking, is another valuable paradigm which we have used before (24,41,42). During a 10-minute trial, *Vglut2*$^{f/f;Emx1\text{-}Cre}$ cKO and control mice were analysed in the EPM. The number of entries (frequency) into each area; i.e. the centre, the closed, and the inner and outer segments of the open arm were scored (Figure 4D), as was the time spent (duration) in each of these compartments (Figure 4D). No differences in either total activity (the sum of all frequencies) in the maze ($P = 0.84$) or in any other parameter were identified (centre frequency, $P = 0.83$; closed arm frequency, $P = 0.60$; inner arm frequency, $P = 0.57$; outer arm frequency,

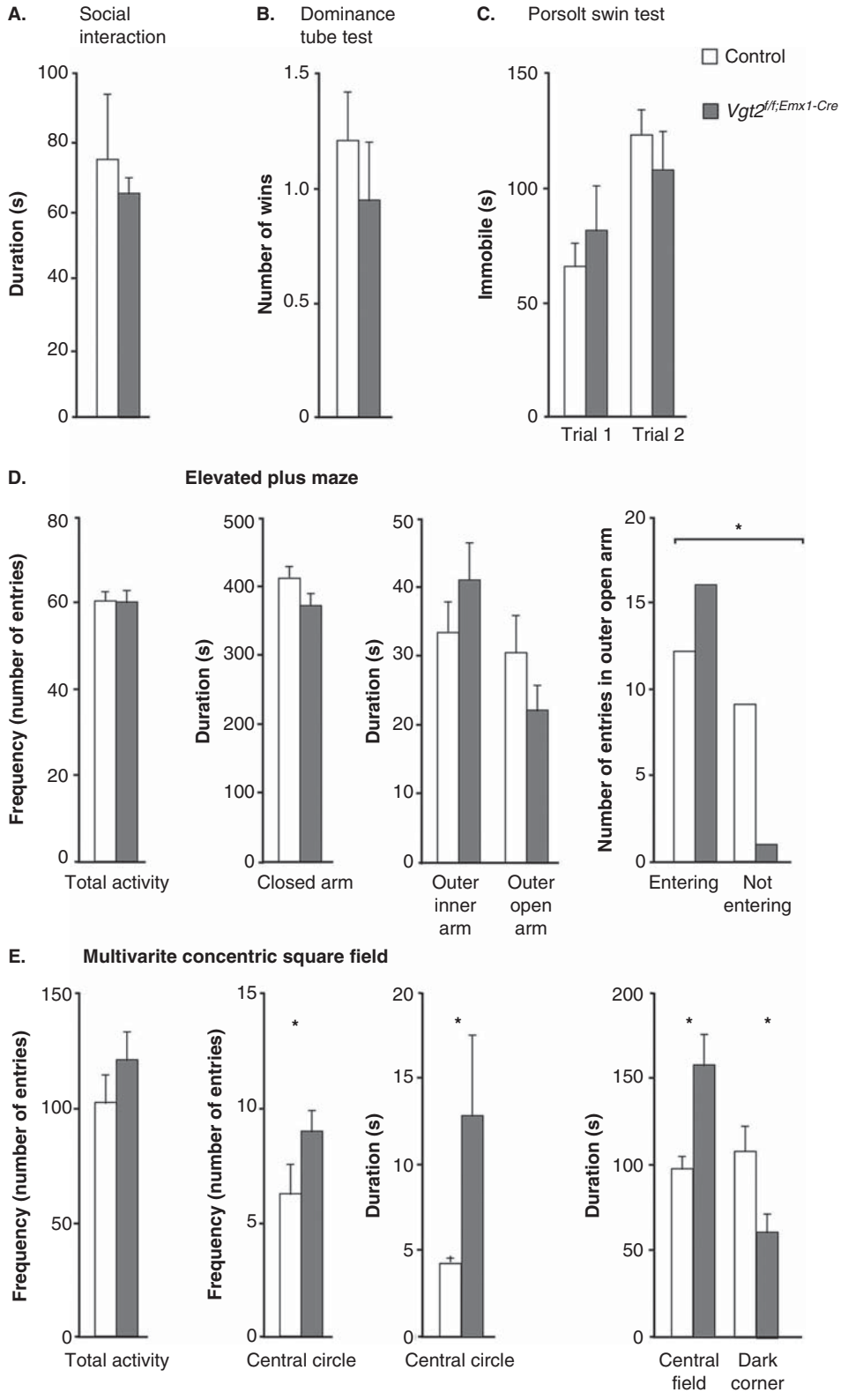

Figure 4. No social deficits or altered despair-like behaviour, but decreased avoidance of open areas and time spent sheltered. Social behaviour analysis on adult *Vglut2*$^{f/f;Emx1\text{-}Cre}$ cKO mice and control littermates (A, B). The total time spent interacting during a 10-min social interaction session shows no alteration in the *Vglut2*$^{f/f;Emx1\text{-}Cre}$ cKO mice compared to control mice (A). The number of wins in the social dominance tube test shows that the *Vglut2*$^{f/f;Emx1\text{-}Cre}$ cKO mice do not display any altered dominance compared to control (B). The *Vglut2*$^{f/f;Emx1\text{-}Cre}$ mice spent equal time swimming during two 12 min swimming sessions separated 24 h apart in the Porsolt swim test (C). The total activity and the duration in the three different areas in the elevated plus maze show no significant differences between genotypes. The number of total entries in the outer open arm is statistically different between the *Vglut2*$^{f/f;Emx1\text{-}Cre}$ cKO mice compared to control mice (*$P < 0.05$, chi-square test) (D). The total activity as measured in the multivariate concentric square field (MCSF) shows no altered behaviour for the *Vglut2*$^{f/f;Emx1\text{-}Cre}$ cKO mice compared to control mice. The frequency in the central circle and duration in the central circle as well as in central field are significantly increased for the *Vglut2*$^{f/f;Emx1\text{-}Cre}$ mice compared to control mice; the duration in the dark corner is significantly decreased in the *Vglut2*$^{f/f;Emx1\text{-}Cre}$ cKO mice compared to control mice (E). Values represent mean ± SEM. * $P < 0.05$ compared to control littermates. cKO = conditional knock-out.

$P = 0.39$; centre time, $P = 0.20$; closed arm time, $P = 0.77$; inner open arm time, $P = 0.28$; and outer open arm time; $P = 0.65$). However, when analysing the number of mice that entered the outer open arm, we found that significantly more cKO than control mice actually visited this exposed area (chi-square, $P = 0.010$) (Figure 4D). To analyse this putatively anxiolytic phenotype further, we turned to the MCSF paradigm (all statistical data are shown in Supplementary Table S3, available online). While displaying the same overall activational level as the controls (Figure 4E), the *Vglut2*$^{f/f;Emx1\text{-}Cre(tg/wt)}$ cKO mice showed a significantly decreased avoidance of the open areas as displayed by higher frequency of visits in the central circle and the time spent there (Figure 4E). The cKO mice also displayed decreased shelter-seeking in the dark room and increased time in the central field. Decreased avoidance of open areas and of the dark room were previously identified in the *Vglut2*$^{f/f;CaMKII\text{-}Cre}$ cKO mice which also showed a general hyperactivity and increased risk-assessment and exploratory behaviour. Compared to the *Vglut2*$^{f/f;CaMKII\text{-}Cre}$ cKO mice, the *Vglut2*$^{f/f;Emx1\text{-}Cre}$ cKO mice thus show a milder behavioural phenotype, but one which is more specifically centred around anxiolysis instead of strong hyperactivity in several different aspects. Taken together, the behavioural alterations identified in the EPM and the MCSF show that the *Vglut2*$^{f/f;Emx1\text{-}Cre}$ cKO mice have an anxiolytic phenotype.

Discussion

Contrary to the strong behavioural phenotype observed when *Vglut2* was gene-targeted in the forebrain from postnatal week 3 and onwards (*Vglut2*$^{f/f;CamKII\text{-}Cre}$ mouse line) (13), the embryonic onset of deletion used in the current study (the *Vglut2*$^{f/f;Emx1\text{-}Cre}$ mouse line) produced a milder behavioural phenotype focused around anxiolysis. As *Vglut2* is broadly expressed in the embryonic mouse brain, including within the dorsal telencephalon (16,17), the embryonal gene targeting in the current study is likely to affect brain development and adult function profoundly differently than a targeting event occurring from 3 weeks of age. Further, the earlier temporal onset of *Vglut2* deletion in the *Vglut2*$^{f/f;Emx1\text{-}Cre}$ mouse line (E10.5 onwards) compared to the *Vglut2*$^{f/f;CamKII\text{-}Cre}$ mouse line (P20 onwards) might lead to the milder behavioural phenotype due to compensations made possible during embryogenesis, but which fail to rescue functions in the postnatal life. In addition to developmental differences between the *Vglut2*$^{f/f;CamKII\text{-}Cre}$ and the *Vglut2*$^{f/f;Emx1\text{-}Cre}$ transgenic mouse lines, an important factor that may contribute to the identified permutations is the genetic background of the mice. Although both kept on a hybrid of C57/BL6J and Sv129, the exact quantity of each contributor is difficult to ascertain. However, as the cKO mice of each line are compared to littermate control mice of the identical genetic background, the impact of genetic background for the overall interpretation of the result is limited.

Importantly, although the spatial extent of gene targeting appeared the same in the neocortex, subiculum, and olfactory bulb in the cKO mice of both the *Vglut2*$^{f/f;Emx1\text{-}Cre}$ and *Vglut2*$^{f/f;CamKII\text{-}Cre}$ mouse lines, *Vglut2* expression was somewhat differentially targeted within the amygdaloid subnuclei. In the *Vglut2*$^{f/f;CamKII\text{-}Cre}$ cKO mice, all amygdaloid expression of *Vglut2* was lacking as identified by our previous ISH analysis (13). In the *Vglut2*$^{f/f;Emx1\text{-}Cre}$ cKO mice, on the other hand, only the *Vglut2* expression in the BM amygdala was completely lacking, while expression in the ACo nucleus was merely blunted and the Me amygdala showed normal *Vglut2* expression. This observation shows that the spatial activity within the amygdala differs between the *Emx1-Cre* and the *CamKII-Cre* transgenes. The amygdaloid complex, consisting of a series of heterogeneous subnuclei, is known to be important for aspects of both fear and anxious behaviour. Anxiety, experienced as unease, dread, apprehension, and similar, is a negative-valenced emotion characterized by sustained hyperarousal in response to uncertainty (42-44). Experienced by all individuals, anxiety serves to guide decision-making by contributing to evaluation of risk and need for defence or avoidance. When anxiety becomes excessive or pathological, however, it may lead up to the substantial group of anxiety disorders that include generalized anxiety disorder and obsessive-compulsive disorder (42,44). A vast number of studies have shown that patients with various kinds of anxiety disorder show amygdala hyperactivity in response to anxiogenic stimuli, leading to the view of amygdala hyperfunction as a key component of human anxiety disorder (45-49). The contribution of specific amygdaloid subnuclei is not firmly established yet, but both inhibitory and excitatory amygdaloid nuclei are implicated in the neurocircuitry of anxiety. In the mouse, the excitatory subnuclei express either *Vglut1* or *Vglut2*, or both, as shown above. The interconnectivity between the amygdaloid nuclei has been investigated thoroughly (described in detail in (50)). The lateral (L; *Vglut1*-expressing) and the Me (*Vglut1*/*Vglut2*-expressing) nuclei send reciprocal projections to the basal (B) and accessory basal (BA) amygdaloid nuclei, which also receive an excitatory drive from the subiculum (*Vglut1*/*Vglut2*-expressing). Excitatory BL amygdala (*Vglut1*) and

local inhibitory projections gate the activity of the inhibitory nucleus central amygdala which in turn projects out from the amygdala to brain-stem, basal forebrain, and hypothalamus regions that control autonomic, hormonal, and behavioural responses to emotional situations. Additional connectivity between the above-mentioned amygdaloid nuclei is also substantially involved in the regulation of emotional responses, which were only briefly summarized here for an overview of *Vglut1* and *Vglut2* expression. Although a *Vglut2*-expressing nucleus, the Me amygdala was not targeted in the $Vglut2^{f/f;Emx1\text{-}Cre}$ cKO mice due to the lack of Emx-Cre-activity in this particular nucleus; thus the anxiolytic phenotype of these cKO mice cannot be attributed to a loss of excitatory drive from this specific subnucleus. On the other hand, the Me nucleus was *Vglut2*-targeted in the $Vglut2^{f/f;CamKII\text{-}Cre}$ cKO mice, possibly explaining the more profound anxiolytic phenotype in these mice, which included increased risk-taking. In the $Vglut2^{f/f;Emx1\text{-}Cre}$ cKO mice, *Vglut2* was deleted in the BM amygdala and partly in the ACo. Further studies would be required to reveal if the loss of *Vglut2* in these particular areas contributes to the observed behavioural phenotypes. Importantly, based on the rather broad deletion of *Vglut2* in the entire telencephalon during embryonal development, it is conceivable that the cause of the anxiolytic phenotype is independent on the restricted targeting of *Vglut2* in the BMA and ACo. For example, as mentioned above, the importance of the subiculum, which expresses both *Vglut1* and *Vglut2* and which we show is lacking *Vglut2* in the cKO mice (both in the $Vglut2^{f/f;CamKII\text{-}Cre}$ and $Vglut2^{f/f;Emx1\text{-}Cre}$ mouse lines), should not be neglected. The subiculum innervates the B/BA amygdaloid nuclei, and loss of *Vglut2* in this hippocampal area may substantially decrease the glutamatergic drive into the amygdala, altering the final balance of output from the CeA so that the level of anxiety is measurably decreased. Hippocampus function in the cKO mice of a similar $Vglut2^{f/f;Emx1\text{-}Cre}$ mouse line was in fact previously shown to be characterized by reduced evoked glutamatergic transmission and release probability in the CA3-CA1 region (51), a feature that might also contribute to the anxiolytic phenotype.

Further addressing the functional roles ascribed to the amygdaloid nuclei expressing *Vglut2*, the BM, M, and ACo amygdala nuclei have all been shown to mediate feeding behaviour via extensive connectivity directly with e.g. the hypothalamus (52,53). No alteration in body weights were observed in our cKO mice, an observation which, taken together with the normal extent of spontaneous activity, indicates a normal amount of food intake.

In summary, the main findings of the current study indicate that expression of *Vglut2* in the dorsal telencephalic area from mid-gestation is not of major importance for establishing the general activational level, responsiveness to the psychostimulant amphetamine, or for sociability, behaviours that all are affected when *Vglut2* is removed in the same areas during adolescence. However, expression of *Vglut2* in the dorsal telencephalic area from mid-gestation is shown to be involved in the regulation of anxiety, possibly by providing excitatory input into the amygdala or by ascertaining a balanced intra-amygdaloid connectivity. Given this restricted behavioural phenotype, the $Vglut2^{f/f;Emx1\text{-}Cre}$ mouse line might be considered a useful tool for further analysis of the neurocircuitry and neurobiology of anxiety.

Acknowledgements

The authors thank Professor Klas Kullander, Uppsala University, for constructive input during the initiation of this study; Professor Kevin Jones, University of Colorado-Boulder, and Professor Rudiger Klein, Max-Planck Institute for Neurobiology, for providing the Emx-Cre mouse line. We thank Dr Carolina Birgner, Uppsala University, for performing the HPLC analysis, and Drs Daniel Andersson and Erik Stuber, both at Gothenburg University, for providing technical expertise in HPLC analysis and behaviour analysis, respectively. Funding: This work was supported by grants from the Swedish Medical Research Council (2007-5742, 2011-4747), Uppsala University, the Swedish Brain Foundation, the Hållsten Research Foundation, and the foundations of Åke Wiberg and Åhlén.

Declaration of interest: The authors report no conflicts of interest. The authors alone are responsible for the content and writing of the paper.

References

1. Nakagawa T, Kaneko S. SLC1 glutamate transporters and diseases: psychiatric diseases and pathological pain. Curr Mol Pharmacol. 2013;6:66–73.
2. Kantrowitz J, Javitt DC. Glutamatergic transmission in schizophrenia: from basic research to clinical practice. Curr Opin Psychiatry. 2012;25:96–102.
3. McCullumsmith RE, Hammond J, Funk A, Meador-Woodruff JH. Recent advances in targeting the ionotropic glutamate receptors in treating schizophrenia. Curr Pharm Biotechnol. 2012;13:1535–42.
4. Spanagel R, Vengeliene V. New pharmacological treatment strategies for relapse prevention. Curr Top Behav Neurosci. 2013;13:583–609.

5. Bellocchio EE, Reimer RJ, Fremeau RT, Edwards RH. Uptake of glutamate into synaptic vesicles by an inorganic phosphate transporter. Science. 2000;289:957–60.
6. Fremeau RT, Burman J, Qureshi T, Tran CH, Proctor J, Johnson J, et al. The identification of vesicular glutamate transporter 3 suggests novel modes of signaling by glutamate. Proc Natl Acad Sci USA. 2002;99:14488–93.
7. Fremeau RT Jr, Troyer MD, Pahner I, Nygaard GO, Tran CH, Reimer RJ, et al. The expression of vesicular glutamate transporters defines two classes of excitatory synapse. Neuron. 2001;31:247–60.
8. Herzog E, Bellenchi GC, Gras C, Bernard V, Ravassard P, Bedet C, et al. The existence of a second vesicular glutamate transporter specifies subpopulations of glutamatergic neuron. J Neurosci. 2001;21:RC181.
9. Kaneko T, Fujiyama F. Complementary distribution of vesicular glutamate transporters in the central nervous system. Neurosci Res. 2002;42:243–50.
10. Takamori S, Rhee JS, Rosenmund C, Jahn R. Identification of a vesicular glutamate transporter that defines a glutamatergic phenotype in neurons. Nature. 2000;407:189–94.
11. Hisano S, Hoshi K, Ikeda Y, Maruyama D, Kanemoto M, Ichijo H, et al. Regional expression of a gene encoding a neuron-specific Na(+)-dependent inorganic phosphate cotransporter (DNPI) in the rat forebrain. Brain Res Mol Brain Res. 2000;83:34–43.
12. Nakamura K, Hioki H, Fujiyama F, Kaneko T. Postnatal changes of vesicular glutamate transporter (VGluT)1 and VGluT2 immunoreactivities and their colocalization in the mouse forebrain. J Comp Neurol. 2005;492:263–88.
13. Wallen-Mackenzie A, Nordenankar K, Fejgin K, Lagerstrom MC, Emilsson L, Fredriksson R, et al. Restricted cortical and amygdaloid removal of vesicular glutamate transporter 2 in preadolescent mice impacts dopaminergic activity and neuronal circuitry of higher brain function. J Neurosci. 2009;29:2238–51.
14. Ohmomo H, Ina A, Yoshida S, Shutoh F, Ueda S, Hisano S. Postnatal changes in expression of vesicular glutamate transporters in the main olfactory bulb of the rat. Neuroscience. 2009;160:419–26.
15. Poulin JF, Castonguay-Lebel Z, Laforest S, Drolet G. Enkephalin co-expression with classic neurotransmitters in the amygdaloid complex of the rat. J Comp Neurol. 2008; 506:943–59.
16. Birgner C, Nordenankar K, Lundblad M, Mendez JA, Smith C, le Greves M, et al. VGLUT2 in dopamine neurons is required for psychostimulant-induced behavioral activation. Proc Natl Acad Sci USA. 2010;107:389–94.
17. Nordenankar K, Smith-Anttila CJ, Schweizer N, Viereckel T, Birgner C, Mejia-Toiber J, et al. Increased hippocampal excitability and impaired spatial memory function in mice lacking VGLUT2 selectively in neurons defined by tyrosine hydroxylase promoter activity. Brain Struct Funct. 2014;Epub ahead of print.
18. Fremeau RT Jr, Voglmaier S, Seal RP, Edwards RH. VGLUTs define subsets of excitatory neurons and suggest novel roles for glutamate. Trends Neurosci. 2004;27:98–103.
19. Boulland J-L, Qureshi T, Seal RP, Rafiki A, Gundersen V, Bergersen LH, et al. Expression of the vesicular glutamate transporters during development indicates the widespread corelease of multiple neurotransmitters. J Comp Neurol. 2004;480:264–80.
20. Gras C, Vinatier J, Amilhon B, Guerci A, Christov C, Ravassard P, et al. Developmentally regulated expression of VGLUT3 during early post-natal life. Neuropharmacology. 2005;49:901–11.
21. Garcia-Garcia AL, Elizalde N, Matrov D, Harro J, Wojcik SM, Venzala E, et al. Increased vulnerability to depressive-like behavior of mice with decreased expression of VGLUT1. Biol Psychiatry. 2009;66:275–82.
22. Tordera RM, Totterdell S, Wojcik SM, Brose N, Elizalde N, Lasheras B, et al. Enhanced anxiety, depressive-like behaviour and impaired recognition memory in mice with reduced expression of the vesicular glutamate transporter 1 (VGLUT1). Eur J Neurosci. 2007;25:281–90.
23. Moechars D, Weston MC, Leo S, Callaerts-Vegh Z, Goris I, Daneels G, et al. Vesicular glutamate transporter VGLUT2 expression levels control quantal size and neuropathic pain. J Neurosci. 2006;26:12055–66.
24. Wallen-Mackenzie A, Gezelius H, Thoby-Brisson M, Nygard A, Enjin A, Fujiyama F, et al. Vesicular glutamate transporter 2 is required for central respiratory rhythm generation but not for locomotor central pattern generation. J Neurosci. 2006;26:12294–307.
25. Wallen-Mackenzie A, Wootz H, Englund H. Genetic inactivation of the vesicular glutamate transporter 2 (VGLUT2) in the mouse: what have we learnt about functional glutamatergic neurotransmission? Ups J Med Sci. 2010;115:11–20.
26. El Mestikawy S, Wallen-Mackenzie A, Fortin GM, Descarries L, Trudeau LE. From glutamate co-release to vesicular synergy: vesicular glutamate transporters. Nat Rev Neurosci. 2011;12:204–16.
27. Alsio J, Nordenankar K, Arvidsson E, Birgner C, Mahmoudi S, Halbout B, et al. Enhanced sucrose and cocaine self-administration and cue-induced drug seeking after loss of VGLUT2 in midbrain dopamine neurons in mice. J Neurosci. 2011;31:12593–603.
28. Hnasko TS, Chuhma N, Zhang H, Goh GY, Sulzer D, Palmiter RD, et al. Vesicular glutamate transport promotes dopamine storage and glutamate corelease in vivo. Neuron. 2010;65:643–56.
29. Fortin GM, Bourque MJ, Mendez JA, Leo D, Nordenankar K, Birgner C, et al. Glutamate corelease promotes growth and survival of midbrain dopamine neurons. J Neurosci. 2012;32:17477–91.
30. Minichiello L, Korte M, Wolfer D, Kuhn R, Unsicker K, Cestari V, et al. Essential role for TrkB receptors in hippocampus-mediated learning. Neuron. 1999;24:401–14.
31. Gorski JA, Talley T, Qiu M, Puelles L, Rubenstein JL, Jones KR. Cortical excitatory neurons and glia, but not GABAergic neurons, are produced in the Emx1-expressing lineage. J Neurosci. 2002;22:6309–14.
32. Crusio WE. Flanking gene and genetic background problems in genetically manipulated mice. Biol Psychiatry. 2004;56: 381–5.
33. Wolfer DP, Crusio WE, Lipp HP. Knockout mice: simple solutions to the problems of genetic background and flanking genes. Trends Neurosci. 2002;25:336–40.
34. Lindgren HS, Andersson DR, Lagerkvist S, Nissbrandt H, Cenci MA. L-DOPA-induced dopamine efflux in the striatum and the substantia nigra in a rat model of Parkinson's disease: temporal and quantitative relationship to the expression of dyskinesia. J Neurochem. 2010;112:1465–76.
35. Elverfors A, Pileblad E, Lagerkvist S, Bergquist F, Jonason J, Nissbrandt H. 3-Methoxytyramine formation following monoamine oxidase inhibition is a poor index of dendritic dopamine release in the substantia nigra. J Neurochem. 1997; 69:1684–92.

36. Porsolt RD, Brossard G, Hautbois C, Roux S. Rodent models of depression: forced swimming and tail suspension behavioral despair tests in rats and mice. Curr Protoc Neurosci. 2001; Chapter 8:Unit 8. 10A.
37. Cryan JF, Mombereau C. In search of a depressed mouse: utility of models for studying depression-related behavior in genetically modified mice. Mol Psychiatry. 2004;9: 326–57.
38. Stornetta RL, Sevigny CP, Schreihofer AM, Rosin DL, Guyenet PG. Vesicular glutamate transporter DNPI/ VGLUT2 is expressed by both C1 adrenergic and nonaminergic presympathetic vasomotor neurons of the rat medulla. J Comp Neurol. 2002;444:207–20.
39. Le Moal M, Simon H. Mesocorticolimbic dopaminergic network: functional and regulatory roles. Physiol Rev. 1991; 71:155–234.
40. Engin E, Treit D. The effects of intra-cerebral drug infusions on animals' unconditioned fear reactions: a systematic review. Prog Neuropsychopharmacol Biol Psychiatry. 2008;32:1399–419.
41. Meyerson BJ, Augustsson H, Berg M, Roman E. The concentric square field: a multivariate test arena for analysis of explorative strategies. Behav Brain Res. 2006; 168:100–13.
42. Sylvers P, Lilienfeld SO, LaPrairie JL. Differences between trait fear and trait anxiety: implications for psychopathology. Clin Psychol Rev. 2011;31:122–37.
43. McNaughton N, Corr PJ. A two-dimensional neuropsychology of defense: fear/anxiety and defensive distance. Neurosci Biobehav Rev. 2004;28:285–305.
44. Graham BM, Milad MR. The study of fear extinction: implications for anxiety disorders. Am J Psychiatry. 2011;168: 1255–65.
45. Etkin A, Wager TD. Functional neuroimaging of anxiety: a meta-analysis of emotional processing in PTSD, social anxiety disorder, and specific phobia. Am J Psychiatry. 2007;164:1476–88.
46. Furmark T, Tillfors M, Marteinsdottir I, Fischer H, Pissiota A, Langstrom B, et al. Common changes in cerebral blood flow in patients with social phobia treated with citalopram or cognitive-behavioral therapy. Arch Gen Psychiatry. 2002;59:425–33.
47. Sah P, Faber ES, Lopez De Armentia M, Power J. The amygdaloid complex: anatomy and physiology. Physiol Rev. 2003;83:803–34.
48. Blair K, Shaywitz J, Smith BW, Rhodes R, Geraci M, Jones M, et al. Response to emotional expressions in generalized social phobia and generalized anxiety disorder: evidence for separate disorders. Am J Psychiatry. 2008;165:1193–202.
49. Bruhl AB, Rufer M, Delsignore A, Kaffenberger T, Jancke L, Herwig U. Neural correlates of altered general emotion processing in social anxiety disorder. Brain Res. 2011;1378: 72–83.
50. Forster GL, Novick AM, Scholl JL, Watt MJ. The role of the amygdala in anxiety disorders. In Ferry B, editor. The amygdala—a discrete multitasking manager. 2012. doi: 10.5772/50323.
51. He H, Mahnke AH, Doyle S, Fan N, Wang CC, Hall BJ, et al. Neurodevelopmental role for VGLUT2 in pyramidal neuron plasticity, dendritic refinement, and in spatial learning. J Neurosci. 2012;32:15886–901.
52. Price JL. Comparative aspects of amygdala connectivity. Ann N Y Acad Sci. 2003;985:50–8.
53. Canteras NS, Simerly RB, Swanson LW. Organization of projections from the medial nucleus of the amygdala: a PHAL study in the rat. J Comp Neurol. 1995;360:213–45.

Supplementary material available online

Supplementary Table S1.
Supplementary Table S2.
Supplementary Table S3.